Crack path prediction in brittle solids by a new discontinuous-like FE approach

Andrea Carpinteri, Roberto Brighenti, Andrea Spagnoli, Sabrina Vantadori

Department of Civil and Environmental Engineering & Architecture, University of Parma, Viale G.P. Usberti 181/A, 43100 Parma, Italy, brigh@unipr.it

ABSTRACT. *The numerical prediction of crack paths in brittle or quasi-brittle solids is difficult from a computational point of view, and non-uniqueness of the solution can occur. To solve such a problem, several computational techniques have been proposed such as ad hoc remeshing strategies, strain softening in the context of plasticity, discontinuous finite elements. In the present paper, a continuum finite element (FE) formulation to model the discontinuity of the displacement field in fracture occurring in brittle or quasi-brittle solids is proposed. A homogeneous discontinuity is assumed to exist in a cracked finite element, and a new simple stress-based implementation of the displacement discontinuity is introduced by an appropriate stress field relaxation in order to simulate the mechanical effects of the crack. The model requires the definition of crack-bridging stress laws. Simple 2D fracture problems are solved to investigate some computational aspects of the proposed algorithm, such as the mesh independence. Finally, the developed numerical model is used to simulate experimental results.*

INTRODUCTION

As is well-known, the numerical simulation of the mechanical behaviour of brittle solids or structures can be difficult because of the strain localisation due to crack formation, when the strength of the material is exceeded in some parts of the solid. The formation of a discontinuity in a solid can produce computational instabilities or even problem divergence which can cause non-uniqueness of the solution [1-3].

Furthermore, the numerical simulation of the strain localisation phenomena usually shows a strong mesh-dependence [4], and some specific strategies or corrections to standard approaches must be introduced: remeshing, mesh adaptivity [1, 5-7], finite element enrichment [8, 9], use of interface elements [10, 11], discontinuous FE formulations [12-16]. Among such approaches, the discontinuous FE displacement field approach has shown to be a simple and useful tool.

In the present paper, a stress-based finite element formulation is proposed to represent embedded discontinuities which usually occur in the fracture process of brittle or quasi-brittle solids and structures. A new simple implementation of the mechanical effects of a discontinuous displacement field within an element is formulated. By introducing an appropriate FE stress field correction at the Gauss point level, the mechanical effects of the opening and sliding stresses transmitted across the crack faces

can be represented in a way similar to that employed in standard plasticity-like FE numerical approaches. The present formulation does not introduce discontinuous or modified shape functions to reproduce strain localisation, but it simply relaxes the stress field in an appropriate fashion by considering crack bridging and shearing laws to evaluate the normal and tangential stresses transmitted across the crack faces. Furthermore, the uncracked material is allowed to behave as a linear elastic or an elastic-plastic one.

The proposed approach is presented in the context of a variational FE formulation. Then, the behaviour of brittle structures as well as the crack paths inside the material in 2D problems are predicted. Finally, some comparisons with literature and experimental results are discussed to assess the capability of this approach.

DISCONTINUOUS FORMULATION

The discontinuous displacement field in a solid Ω (Fig. 1a) where a displacement discontinuity takes place along the line S can be written as follows [12]:

$$\boldsymbol{\delta}(\mathbf{x}) = \bar{\boldsymbol{\delta}}(\mathbf{x}) + H(\mathbf{x})[[\boldsymbol{\delta}(\mathbf{x})]] = \bar{\boldsymbol{\delta}}(\mathbf{x}) + \underbrace{H(\mathbf{x}) \cdot \mathbf{w}(\mathbf{x})}_{\boldsymbol{\delta}_d(\mathbf{x})} \tag{1}$$

where the total displacement field $\boldsymbol{\delta}(\mathbf{x})$ is written as the sum of the continuous $\bar{\boldsymbol{\delta}}(\mathbf{x})$ and the discontinuous part $\boldsymbol{\delta}_d(\mathbf{x}) = H(\mathbf{x})[[\boldsymbol{\delta}(\mathbf{x})]] = H(\mathbf{x}) \cdot \mathbf{w}(\mathbf{x})$ (where $H(\mathbf{x})$ is the Heaviside jump function across the crack line, and $[[\boldsymbol{\delta}(\mathbf{x})]] = \mathbf{w}(\mathbf{x})$ is the discontinuity displacement jump vector across the line S). The corresponding strain field is given by:

$$\boldsymbol{\varepsilon}(\mathbf{x}) = \underbrace{\nabla^s \bar{\boldsymbol{\delta}}(\mathbf{x}) + H(\mathbf{x}) \cdot \nabla^s \mathbf{w}(\mathbf{x})}_{\boldsymbol{\varepsilon}^b(\mathbf{x})} + \underbrace{\delta_s \left(\mathbf{w}(\mathbf{x}) \otimes \mathbf{i}\right)^s}_{\boldsymbol{\varepsilon}^u(\mathbf{x})} \tag{2}$$

where δ_s is the Dirac delta function in S, $(\bullet)^s$ denotes the symmetric part of $(\bullet)$, $\boldsymbol{\varepsilon}^b(\mathbf{x})$ and $\boldsymbol{\varepsilon}^u(\mathbf{x})$ are the bounded and unbounded part of the strains, respectively.

By considering a finite element (Fig. 1b), in which a discontinuity occurs along a straight line S crossing the element in a direction identified by the unit vector $\mathbf{j}$ and centred in its geometrical centre C, the displacement field $\mathbf{u}(\mathbf{x})$ can be written [12, 16]:

$$\mathbf{u}(\mathbf{x}) = \mathbf{N}(\mathbf{x}) \cdot \boldsymbol{\delta} + \left[H(\mathbf{x}) - \mathbf{N}^+(\mathbf{x})\right]\mathbf{w} \tag{3}$$

where the discontinuous part is given by $\left[H(\mathbf{x}) - \mathbf{N}^+(\mathbf{x})\right]\mathbf{w}$. The displacement jump vector is $\mathbf{w} = \mathbf{u} + \mathbf{v}$, where $\mathbf{u}$ and $\mathbf{v}$ are the displacements jumps normal and parallel to the crack line, respectively (Fig. 1b).

The corresponding small strain field can be obtained from:

$$\boldsymbol{\varepsilon}(\mathbf{x}) = \underbrace{\mathbf{B}(\mathbf{x})\boldsymbol{\delta}(\mathbf{x}) - \left[\mathbf{B}^+(\mathbf{x}) \otimes \mathbf{w}(\mathbf{x})\right]^s}_{\boldsymbol{\varepsilon}^b(\mathbf{x})} + \underbrace{\delta_s \mathbf{w}(\mathbf{x})}_{\boldsymbol{\varepsilon}^u(\mathbf{x})} \quad \text{with} \quad \mathbf{B}^+(\mathbf{x}) = \sum_{i \in \Omega_e^+} B_i(\mathbf{x}) \tag{4}$$

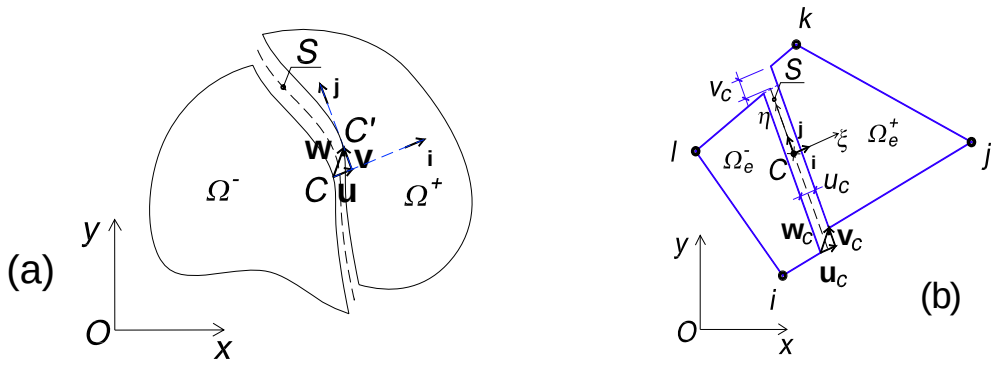

Figure 1. (a) Discontinuous displacement field in a 2-D solid; (b) Schematisation in a F.E.

where $\mathbf{B}(\mathbf{x})$ is the compatibility matrix. In the above expression, the crack jump displacement vector $\mathbf{w}(\mathbf{x})$ is unknown, and must be evaluated by taking into account the material cohesive crack bridging law for the normal and tangential stresses.

VARIATIONAL FORMULATION OF DISCONTINUOUS F.E.

The equilibrium problem can be stated through the following weak form [14]:

$$\int_{\Omega\setminus S} \nabla^s(\delta\mathbf{u}^*)\boldsymbol{\sigma}\,d\Omega = \int_{\Omega\setminus S} \delta\mathbf{u}^*\,\mathbf{b}\,d\Omega + \int_{\Gamma_t} \delta\mathbf{u}^*\,\mathbf{t}\,d\Gamma + \int_{S} (\delta\mathbf{u}^{+*} - \delta\mathbf{u}^{-*})\mathbf{t}^+\,d\Gamma \tag{5}$$

for any virtual displacement field $\delta\mathbf{u}^*$ and corresponding strains and stresses $\delta\boldsymbol{\varepsilon}^* = \nabla^s\delta\mathbf{u}^*$, $\delta\boldsymbol{\sigma}^* = \delta\boldsymbol{\sigma}^*\left(\nabla^s\delta\mathbf{u}^*\right)$. By introducing the FE notation, it can be written as:

$$\begin{aligned}&\int_{\Omega\setminus S} \left[\mathbf{B}\cdot\delta\boldsymbol{\delta}^* - \left[\mathbf{B}^+\otimes\delta\mathbf{w}^*\right]^s\right]\mathbf{C}\left[\mathbf{B}\cdot\boldsymbol{\delta} - \left[\mathbf{B}^+\otimes\mathbf{w}\right]^s\right]d\Omega = \\ &= \int_{\Omega\setminus S} \left[\mathbf{N}\cdot\delta\boldsymbol{\delta}^* + \left[H-\mathbf{N}^+\right]\delta\mathbf{w}^*\right]\mathbf{b}\,d\Omega + \int_{\Gamma_t} \left[\mathbf{N}\cdot\delta\boldsymbol{\delta}^* + \left[H-\mathbf{N}^+\right]\delta\mathbf{w}^*\right]\mathbf{t}\,d\Gamma + \int_{S} \delta\mathbf{w}^*\,\mathbf{t}^+\,d\Gamma\end{aligned} \tag{6}$$

Since the virtual displacements $\delta\mathbf{w}^*$ and $\delta\boldsymbol{\delta}^*$ are arbitrary, we can assume $\delta\mathbf{w}^* = \mathbf{0}$ and $\delta\boldsymbol{\delta}^* = \mathbf{0}$ separately in eq. (6) and get the following expressions, after eliminating the arbitrary displacements $\delta\boldsymbol{\delta}^*$ and the discontinuity vector $\delta\mathbf{w}^*$:

$$\begin{bmatrix} \int_{\Omega\setminus S}\mathbf{B}^t\,\mathbf{C}\mathbf{B}\,d\Omega & -\int_{\Omega\setminus S}\mathbf{B}^t\,\mathbf{C}\mathbf{B}^+\,d\Omega \\ \int_{\Omega\setminus S}\mathbf{B}^{t^+}\mathbf{C}\mathbf{B}\,d\Omega & \int_{\Omega\setminus S}\mathbf{B}^{t^+}\mathbf{C}\mathbf{B}^+\,d\Omega \end{bmatrix} \begin{Bmatrix} \boldsymbol{\delta} \\ \mathbf{w} \end{Bmatrix} = \begin{Bmatrix} \int_{\Omega\setminus S}\mathbf{N}^t\,\mathbf{b}\,d\Omega + \int_{\Gamma_t}\mathbf{N}^t\,\mathbf{t}\,d\Gamma \\ \int_{\Omega\setminus S}\left[H-\mathbf{N}^+\right]^t\,\mathbf{b}\,d\Omega + \int_{\Gamma_t}\left[H-\mathbf{N}^+\right]^t\,\mathbf{t}\,d\Gamma \end{Bmatrix} \tag{7}$$

or, in a compact form, after performing a static condensation:

$$\begin{cases} \mathbf{w} = \mathbf{K}_{ww}^{-1}\left(\mathbf{f}_2 - \mathbf{K}_{w\delta}\boldsymbol{\delta}\right) \\ \boldsymbol{\delta} = \mathbf{K}_{\delta\delta}^{-1}\left(\mathbf{f}_1 - \mathbf{K}_{\delta w}\mathbf{w}\right) = \left(\mathbf{K}_{\delta\delta} - \mathbf{K}_{\delta w}\mathbf{K}_{ww}^{-1}\mathbf{K}_{w\delta}\right)^{-1}\left(\mathbf{f}_1 - \left(\mathbf{K}_{\delta w}\mathbf{K}_{ww}^{-1}\mathbf{K}_{w\delta}\right)\mathbf{f}_2\right) \end{cases} \tag{8}$$

As is stated above, the solution of the problem requires the knowledge of the crack jump displacement vector $\mathbf{w}(\mathbf{x})$.

When a crack starts, it is reasonable to assume that the strain state present in the finite element is "condensed" in a highly-localised strained area concentrated in a very narrow band (crack location), i.e. a discrete displacement jump can be assumed. Let us consider the FE mean nodal displacement values across the crack, projected respectively in direction normal ($\mathbf{u}_c$) and parallel ($\mathbf{v}_c$) to the crack direction:

$$\mathbf{w}_c = \mathbf{u}_c + \mathbf{v}_c = u_c \cdot \mathbf{i} + v_c \cdot \mathbf{j}, \quad \text{with} \quad u_c = \left[\mathbf{Q} \cdot \left(\boldsymbol{\delta} \cdot \mathbf{i}\right)\right] / n_n, \quad v_c = \left[\mathbf{Q} \cdot \left(\boldsymbol{\delta} \cdot \mathbf{j}\right)\right] / n_n \tag{9}$$

where n_n is the total number of element nodes, the matrix $\mathbf{Q}$ is the nodal discontinuity matrix, $\boldsymbol{\delta}$ is the element nodal displacement vector.

The nodal discontinuity matrix $\mathbf{Q}$ is determined by observing which nodes of the finite element are in one or in the other side of the crack. By referring to Fig. 1b:

$$\mathbf{Q} = \begin{bmatrix} \overbrace{-1 \;\; 0}^{node\ i} & \overbrace{+1 \;\; 0}^{node\ j} & \overbrace{+1 \;\; 0}^{node\ k} & \overbrace{-1 \;\; 0}^{node\ l} \\ 0 \;\; -1 & 0 \;\; +1 & 0 \;\; +1 & 0 \;\; -1 \end{bmatrix} \begin{matrix} \\ \leftarrow \text{dofs along } x \\ \leftarrow \text{dofs along } y \end{matrix} \tag{10}$$

To physically represent the presence of the crack, the stress state in the finite element must be modified in order to have exactly the stress σ_c and the stress τ_c transmitted respectively in direction perpendicular and parallel to the crack faces. The stress state can be *elastically-corrected* as follows:

$$\boldsymbol{\sigma}_{rel,u} = \boldsymbol{\sigma} - \mathbf{C} : \left[\nabla^s\left(\mathbf{N} \cdot \boldsymbol{\delta}_{u,s}\right)\right] = \boldsymbol{\sigma} - \mathbf{C} : \left[\nabla^s\left(\mathbf{N} \cdot s_n \cdot \boldsymbol{\delta}_u\right)\right] = \boldsymbol{\sigma} - \mathbf{C} : \left(s_n \cdot \mathbf{B} \cdot \boldsymbol{\delta}_u\right) \tag{11}$$

where $\boldsymbol{\sigma}$ is the effective stress tensor, and $\boldsymbol{\delta}_{u,s} = \left(s_n \cdot \boldsymbol{\delta}_u\right)$ is a fictitious nodal displacement vector assumed to be proportional, through the coefficient s_n, to the nodal displacement vector $\boldsymbol{\delta}_u$. Analogously, by introducing a fictitious displacement vector $\boldsymbol{\delta}_{v,s} = \left(s_s \cdot \boldsymbol{\delta}_v\right)$, which is assumed to be proportional (through the coefficient s_s) to the nodal displacement vector $\boldsymbol{\delta}_v$ obtained by considering the projection $\boldsymbol{\delta}_v = \left(\boldsymbol{\delta} \cdot \mathbf{j}\right) \cdot \mathbf{j}$ of the current nodal displacement vector $\boldsymbol{\delta}$ on the direction $\mathbf{j}$, the stress state becomes:

$$\boldsymbol{\sigma}_{rel,v} = \boldsymbol{\sigma} - \mathbf{C} : \left[\nabla^s\left(\mathbf{N} \cdot \boldsymbol{\delta}_{v,s}\right)\right] = \boldsymbol{\sigma} - \mathbf{C} : \left[\nabla^s\left(\mathbf{N} \cdot s_s \cdot \boldsymbol{\delta}_v\right)\right] = \boldsymbol{\sigma} - \mathbf{C} : \left(s_s \cdot \mathbf{B} \cdot \boldsymbol{\delta}_v\right) \tag{12}$$

The normal stress $\sigma_{c,n}$ and shear stress $\tau_{c,n}$ can be evaluated as follows:

$$\sigma_{c,n} = \left(\boldsymbol{\sigma}_{c,u} \cdot \mathbf{i}\right) \cdot \mathbf{i} = \left[\mathbf{C} : \left(\mathbf{B}' \cdot \boldsymbol{\delta}_{u,s}\right) \cdot \mathbf{i}\right] \cdot \mathbf{i}, \qquad \tau_{c,n} = \left(\boldsymbol{\sigma}_{c,v} \cdot \mathbf{i}\right) \cdot \mathbf{j} = \left[\mathbf{C} : \left(\mathbf{B}' \cdot \boldsymbol{\delta}_{v,s}\right) \cdot \mathbf{i}\right] \cdot \mathbf{j} \tag{13}$$

where $\mathbf{B}'$ is the compatibility matrix evaluated at point C. The effective normal and shear stresses, $\sigma_{e,n}$, $\tau_{e,n}$, acting on the same crack plane but produced by the modified stress tensors $\boldsymbol{\sigma}_{rel,n}$ and $\boldsymbol{\sigma}_{rel,s}$, are expressed as follows:

$$\sigma_{e,n} = \left(\boldsymbol{\sigma}_{rel,n} \cdot \mathbf{i}\right) \cdot \mathbf{i}, \qquad \tau_{s,n} = \left(\boldsymbol{\sigma}_{rel,s} \cdot \mathbf{i}\right) \cdot \mathbf{j} \tag{14}$$

By imposing that $\sigma_{e,n} = \sigma_c(u_c)$ and $\tau_{e,n} = \tau_c(u_c)$, the correction factors s_n, s_s can be determined by writing the corrected stress state at point C:

$$s_n = \frac{(\boldsymbol{\sigma}'\cdot\mathbf{i})\cdot\mathbf{i} - \sigma_c(u_c)}{\left[\left(\mathbf{C}:\mathbf{B}'\cdot\boldsymbol{\delta}_u\right)\cdot\mathbf{i}\right]\cdot\mathbf{i}} = 1 - \frac{\sigma_c(u_c)}{\left[\left(\mathbf{C}:\mathbf{B}'\cdot\boldsymbol{\delta}_u\right)\cdot\mathbf{i}\right]\cdot\mathbf{i}},\ s_s = \frac{(\boldsymbol{\sigma}'\cdot\mathbf{i})\cdot\mathbf{j} - \tau_c(u_c)}{\left[\left(\mathbf{C}:\mathbf{B}'\cdot\boldsymbol{\delta}_v\right)\cdot\mathbf{i}\right]\cdot\mathbf{j}} = 1 - \frac{\tau_c(u_c)}{\left[\left(\mathbf{C}:\mathbf{B}'\cdot\boldsymbol{\delta}_v\right)\cdot\mathbf{i}\right]\cdot\mathbf{j}} \tag{15}$$

and the stress tensor correction (12) becomes

$$\boldsymbol{\sigma}_{rel} = \boldsymbol{\sigma} - \mathbf{C}:\left[\nabla^s\left(\mathbf{N}\cdot\left(\boldsymbol{\delta}_{u,s} + \boldsymbol{\delta}_{v,s}\right)\right)\right] = \boldsymbol{\sigma} - \mathbf{C}:\left[\nabla^s\left(\mathbf{N}\cdot\boldsymbol{\delta}_{w,s}\right)\right] \tag{16}$$

The above stress-based formulation of the discontinuous displacement field can be reinterpreted by a variational approach considering Eq. (5). From eq. (16), we have:

$$\begin{aligned}
&\int_\Omega \nabla^s\left(\delta\mathbf{u}^*\right)\boldsymbol{\sigma}_{rel}\,d\Omega = \int_\Omega \nabla^s\left(\delta\mathbf{u}^*\right)\left\{\boldsymbol{\sigma} - \mathbf{C}:\left[\nabla^s\left(\mathbf{N}\cdot\left(\boldsymbol{\delta}_{w,s}\right)\right)\right]\right\}d\Omega = \int_\Omega \delta\mathbf{u}^*\,\mathbf{b}\,d\Omega + \int_{\Gamma_t} \delta\mathbf{u}^*\,\mathbf{t}\,d\Gamma = \\
&\int_\Omega \delta\boldsymbol{\delta}^{*t}\,\mathbf{B}^t\boldsymbol{\sigma}\,d\Omega = \int_\Omega \delta\boldsymbol{\delta}^{*t}\,\mathbf{B}^t\mathbf{C}\,\mathbf{B}\cdot\boldsymbol{\delta}_{w,s}\,d\Omega + \int_\Omega \delta\boldsymbol{\delta}^{*t}\,\mathbf{N}^t\,\mathbf{b}\,d\Omega + \int_{\Gamma_t} \delta\boldsymbol{\delta}^{*t}\,\mathbf{N}^t\,\mathbf{t}\,d\Gamma
\end{aligned} \tag{17}$$

Since the variation of the displacement field is arbitrary, we obtain:

$$\begin{aligned}
&\int_\Omega \mathbf{B}^t\mathbf{C}\,\mathbf{B}\,d\Omega\boldsymbol{\delta} = \int_\Omega \mathbf{N}^t\,\mathbf{b}\,d\Omega + \int_{\Gamma_t} \mathbf{N}^t\,\mathbf{t}\,d\Gamma + \int_\Omega \mathbf{B}^t\mathbf{C}\,\mathbf{B}\cdot\boldsymbol{\delta}_{w,s}\,d\Omega \qquad \text{i.e.} \\
&\boldsymbol{\delta} = \mathbf{K}^{-1}\left(\mathbf{f}_1 + \mathbf{K}\boldsymbol{\delta}_{w,s}\right)
\end{aligned} \tag{18}$$

From eqs (15), we have:

$$\begin{aligned}
\boldsymbol{\delta}_{w,s} &= \underbrace{\left\{\frac{\sigma_c(u_c)}{\left[\left(\mathbf{C}:\mathbf{B}'\cdot\boldsymbol{\delta}_u\right)\cdot\mathbf{i}\right]\cdot\mathbf{i}} - 1\right\}}_{A}\cdot\mathbf{N}(\mathbf{x})\cdot\boldsymbol{\delta}_u + \underbrace{\left\{\frac{\tau_c(u_c)}{\left[\left(\mathbf{C}:\mathbf{B}'\cdot\boldsymbol{\delta}_v\right)\cdot\mathbf{i}\right]\cdot\mathbf{j}} - 1\right\}}_{B}\cdot\mathbf{N}(\mathbf{x})\cdot\boldsymbol{\delta}_v = \\
&= +\mathbf{N}(\mathbf{x})\left[A(\mathbf{Q},\boldsymbol{\delta},\sigma_c(u_c))\cdot\boldsymbol{\delta}_u + B(\mathbf{Q},\boldsymbol{\delta},\tau_c(u_c))\cdot\boldsymbol{\delta}_v\right]
\end{aligned} \tag{19}$$

and equation (18) can be rewritten as follows:

$$\begin{aligned}
&\int_\Omega \mathbf{B}^t\mathbf{C}\,\mathbf{B}\,d\Omega\boldsymbol{\delta} = \int_\Omega \mathbf{N}^t\,\mathbf{b}\,d\Omega + \int_{\Gamma_t} \mathbf{N}^t\,\mathbf{t}\,d\Gamma + \int_\Omega \mathbf{B}^t\mathbf{C}\,\mathbf{B}\cdot\mathbf{N}\left[A(\mathbf{Q},\boldsymbol{\delta},\sigma_c(u_c))\cdot\boldsymbol{\delta}_u + B(\mathbf{Q},\boldsymbol{\delta},\tau_c(u_c))\cdot\boldsymbol{\delta}_v\right]d\Omega \\
&\text{or}\quad \boldsymbol{\delta} = \mathbf{K}^{-1}\left(\mathbf{f}_1 - \int_\Omega \mathbf{B}^t\mathbf{C}\,\mathbf{B}\cdot\mathbf{N}\left[A(\mathbf{Q},\boldsymbol{\delta},\sigma_c(u_c))\cdot\boldsymbol{\delta}_u + B(\mathbf{Q},\boldsymbol{\delta},\tau_c(u_c))\cdot\boldsymbol{\delta}_v\right]d\Omega\right)
\end{aligned} \tag{20}$$

It can be observed as the last espression in eq.(19) is similar to eq.(3). The discontinuity vector $\boldsymbol{\delta}_{w,s} = \boldsymbol{\delta}_{u,s} + \boldsymbol{\delta}_{v,s}$ must be evaluated by an iterative process summarised in eq. (19).

Crack bridging laws

A cohesive-friction law for the cracked material is assumed in order to simulate the so-called crack process zone. The transmitted stresses are described by a decreasing function of the relative crack face displacement u_c. A decreasing exponential law is adopted for $\sigma_c(u_c)$ [14, 16] and the shear stress $\tau_c(u_c)$:

$$\sigma_c(u_c) = f_t \cdot e^{\frac{2f_t(u_0-u_c)}{2G_f - f_t \cdot u_0}}, \qquad \tau_c(u_c) = \begin{cases} c \cdot \left(1 - \left(\dfrac{u_c}{2 \cdot r_c}\right)^n\right) & \text{if } 0 < u_c < 2 \cdot r_c \\ 0 & \text{if } u_c > 2 \cdot r_c \end{cases} \tag{21}$$

where f_t is the maximum tensile strength, u_0 is the lower crack opening limit at which the bridging process occurs, G_f is the fracture energy of the material [18], and r_c is the crack surface roughness. Equation (21) is governed by the fracture energy of the material, G_f, which represents the dissipated energy per unit crack surface:

$$G_f = \int_{u_0}^{+\infty} f_t \cdot e^{\frac{2f_t(u_0-u_c)}{2G_f - f_t \cdot u_0}} dv \tag{22}$$

Convergence requirements

Since the non-linear computational process involves the evaluation of the crack effects, some appropriate convergence requirements must be considered. The evaluation of the bridging stress is based on the knowledge of the crack opening (CO). In order to control the crack opening convergence, the following crack opening tolerance is introduced:

$$tol_{u_c} = \left| u_c^{(i)} - u_c^{(i-1)} \right| / u_c^{(i)} \tag{23}$$

where $u_c^{(i)}, u_c^{(i-1)}$ are the CO displacements at the iteration *i* and *i*-1, respectively.

NUMERICAL APPLICATION

The algorithm described in the previous sections has been implemented in a non-linear 2-D FE code developed by the authors.

Single-edge notched beam under four-point shear

A four-point shear loaded single-edge notched beam is examined. Such a configuration has been used by several Authors as a benchmark test for numerical analyses [14]. The geometrical parameters of the structure and two FE discretisations are displayed in Fig. 2a, c (sizes in mm). A beam thickness equal to 0.1 m is adopted and a plane stress condition is assumed. The mechanical parameters of the material are: Young modulus $E = 35\,\text{GPa}$, Poisson's ratio $\nu = 0.15$, ultimate tensile strength $f_t = 2.8\,\text{MPa}$, fracture energy $G_F = 100\,\text{N/m}$. A linear-elastic behaviour of the beam is firstly assumed.

The analysis is performed under displacement control. The crack mouth sliding displacement d (CMSD, Fig.2f) is evaluated and represented against the vertical bottom

applied load P in Fig. 2e, together with some results taken from the literature [12, 13].

As can be observed, the load vs CMSD results are in satisfactory agreement with the literature results even if some differences can be appreciated in the decreasing branch of the numerical curves. In Fig. 2e the elastic-plastic case is also shown: the Drucker-Prager plasticity criterion is assumed for the uncracked material with tension (compression) yield stress equal to $\sigma_{Y,t(c)} = 2.8\ (28)\ MPa$, respectively and hardening equal to $H = 0$ (perfect plasticity). As can be observed, the plastic behaviour slightly modifies the load-CMSD curve which has a lower peak with respect to the elastic cases. In Fig. 2b, d, expected crack paths are reproduced by the numerical simulations for the two meshes.

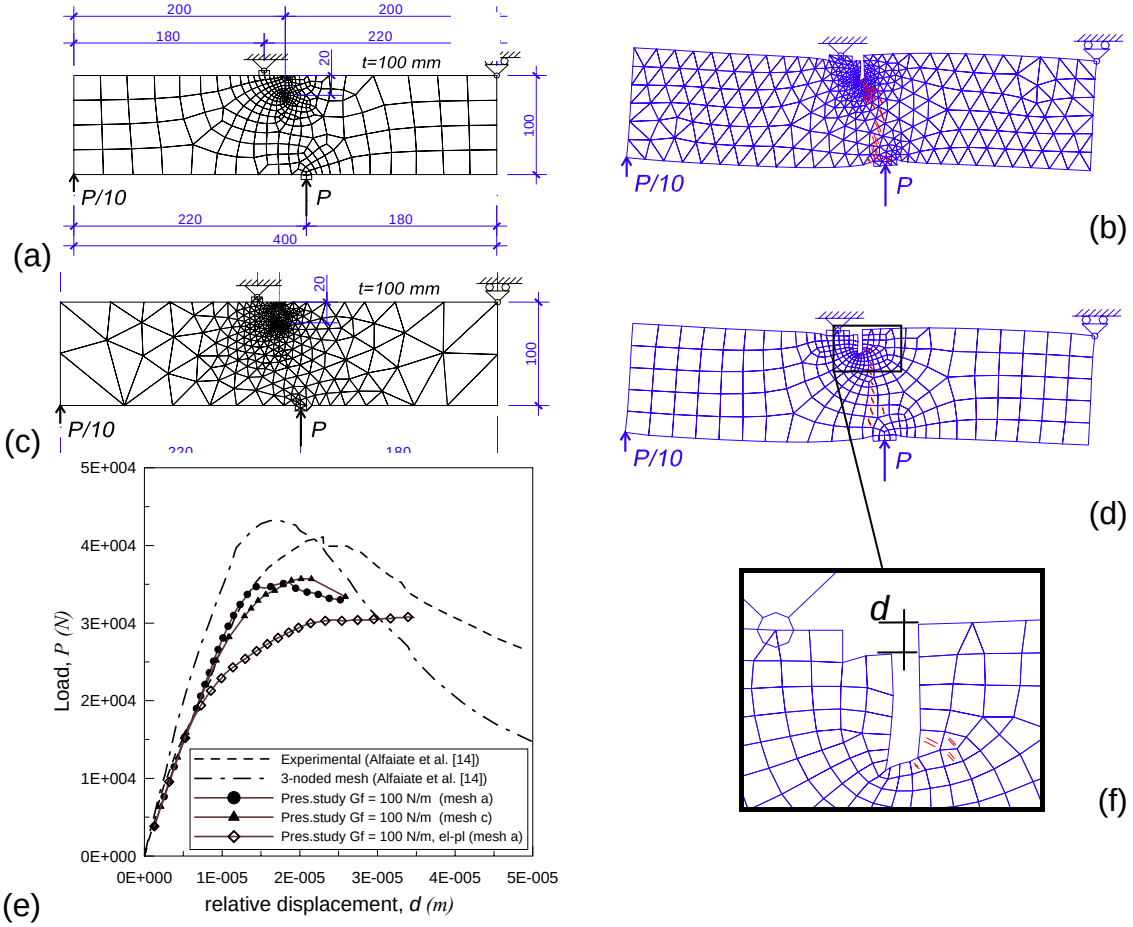

Figure 2. Single-edge notched beam under four point shear: (a) discretisation with 301 4-noded bilinear elements and 343 nodes; (c) discretisation with 660 triangular elements and 378 nodes. (b) Crack path for mesh (a); (d) crack path for mesh (c). Load P vs vertical relative crack displacement (e) and detail of relative crack displacement measurement (f).

CONCLUSIONS

A new continuous finite elements (FE) formulation to simulate strong discontinuity problems, such as the fracture process in brittle or quasi-brittle solids, is herein

presented. A new stress-based implementation of the discontinuous displacement field is proposed by introducing an appropriate stress relaxation to simulate (as usually occurs in classical elastic-plastic FE formulation) the mechanical effects of the cohesive crack in fractured solids or structures. The proposed formulation does not need special discontinuous or modified shape functions to reproduce the discontinuous displacement field, but it simply considers the mechanical (i.e. static) effects of the crack on the body. Both linear elastic and elastic-plastic behaviour of the non-cracked material are considered. The proposed formulation is applied to some 2D problems to assess the capability of the algorithm for simulation of Mode I or mixed Mode I+II fracture problems. The proposed stress-based discontinuous FE formulation gives us results in good agreement with the predictions determined through the classical discontinuous displacement FEs or by experimental tests. Further, it is simple and computationally economic, and preserves the well-known features of the classical elastic-plastic FE formulation.

REFERENCES

1. Tin-Loi, F., Tseng, P. (2003) Comp. Met. in Appl. Mech. and Engng **192,** 1377–1388.
2. Jirásek, M., Belytschko, T. (2002) Proceedings of the Fifth World Congress of Computational Mechanics. WCCM V, Vienna.
3. Carpinteri, A., Spagnoli, A., Vantadori, S. (2005) Mechanical damage of ordinary or prestressed reinforced concrete beams under cyclic bending. Engng Fract. Mech. **72**, 1313-1328.
4. Belytschko, T., Fish, J., Engelmann, B.E. (1988) Comp. Meth. in Appl. Mech. and Engng **70,** 59-89
5. Rashid, M. (1998) Comput. Meth. in Applied Mech. and Engng **154**, 133–150.
6. Bouchard, P.O., Bay, F., Chastel, Y., Tovena, I. (2000) Comp Meth in Appl Mech and Engng **189**, 723–742.
7. Comi, C., Perego, U. (2004) European J of Mech A/Solids **23**, 615–632.
8. Belytschko, T., Black, T. (1999) Int. J. for Num. Meth. In Engng **45**, 601–620.
9. Möes, N., Bolbow, J., Belytschko, T.(1999) Int. J. Num. Meth. In Engng **46**, 131-150.
10. Alfaiate, E.B. Pires, J.A.C. Martins. (1997) Comput. & Struct. **63** 17–26.
11. De Xie, Waas, A.M. (2006) Engng Fract. Mech. **73**, 1783–1796.
12. Oliver, J. (2000) Int. J. of Sol. & Struct. **37**, 7207–7229.
13. Wells, G.N., Sluys, L.J. (2001) Int. J. of Sol. & Struct. **38**, 897–913.
14. Alfaiate, J., Simone, A., Sluys, L.J. (2003) Int. J. of Sol. & Struct. **40**,5799–5817.
15. Oliver, J., Huespe, A.E. (2004) Comp. Meth. Appl. Mech. & Engng **193,** 2987-3014.
16. Sancho, J.M., Planas, J., Cendón, D.A., Reyes, E., Gálvez, J.C. (2007) Engng Fract. Mech. **74**, 75–86.
17. Guo, X.H., Tin-Loi, F., Li, H. (1999) Cement and Concrete Research **29**, 1055-1059.
18. Hillerborg, A., Modéer, M., Peterson, P.E. (1976) Cement and Concrete Research **6**, 773-782.